MODEL-BASED DECISION MAKING TO MANAGE PRODUCTION IN THE WESTERN COMPARTMENT AT ROTOKAWA

Jonathon Clearwater[1], Dario Hernandez[1], Steven Sewell[1,2] and Simon Addison[1]

[1]Mercury NZ Limited; New Zealand

[2] Victoria University; New Zealand

jonathon.clearwater@mercury.co.nz

Keywords: *Rotokawa, Modelling, Reservoir Engineering, Production Engineering, TOUGH2*

ABSTRACT

This paper documents how Mercury NZ Limited used a model-based approach to refine the reservoir management strategy at the Rotokawa geothermal field. We describe the data analysis required to refine our conceptual understanding of the reservoir and how this conceptual model was implemented as a numerical model of a sector in the field known as the Western Compartment. We detail how the diverse datasets from geology, reservoir engineering, geophysics and geochemistry were included to constrain the numerical model forecasts. Tools developed in-house at Mercury were used to run scenarios where changes in surface operations were fed back to the reservoir via a coupled wellbore simulator. Well enthalpies, deliverability curves and decline rates from this coupled numerical model forecast were passed into a decision analysis model using key financial variables. The outcome of this multi-system modelling was a refinement to the reservoir management strategy, namely a reduction in take from the Western Compartment and the decision to locate future make-up production outside of the Compartment.

1. INTRODUCTION

Decision making can be very complex in geothermal fields. Disparate datasets need to be combined into a consistent conceptual understanding of key reservoir processes. The conceptual understanding needs to be transformed into quantitative forecasts of reservoir behavior, including feedback regarding how changes in surface operations influence the subsurface thermodynamics and *vice versa*. Economics needs to be included and uncertainty in forecasts needs to be factored in. This is no trivial task. In Figure 1 we outline some of the tools, business processes and data sources that have been developed and are used by Mercury to guide decision making. In this paper we illustrate how these have been applied to decide on the optimal production strategy following changes in production enthalpy from one sector of the Rotokawa Geothermal Field.

1.1 Background to Rotokawa

The Rotokawa Geothermal Field is located in New Zealand's Taupo Volcanic Zone (TVZ), as shown in Figure 2. Exploration drilling at Rotokawa began in the 1960s. In 1997 the Rotokawa Geothermal Power Station was commissioned. This was originally a 24 MWe Ormat Geothermal Combined Cycle plant which was expanded to 34 MWe in 2003. In 2010 the 138 MWe Sumitomo/Fuji triple-flash Nga Awa Purua power station was commissioned.

The field response to development has been described in a series of papers focused on the conceptual model (Sewell et al., 2015a), numerical model (Hernandez et al., 2015a), reservoir physical response (Hernandez et al., 2015b),

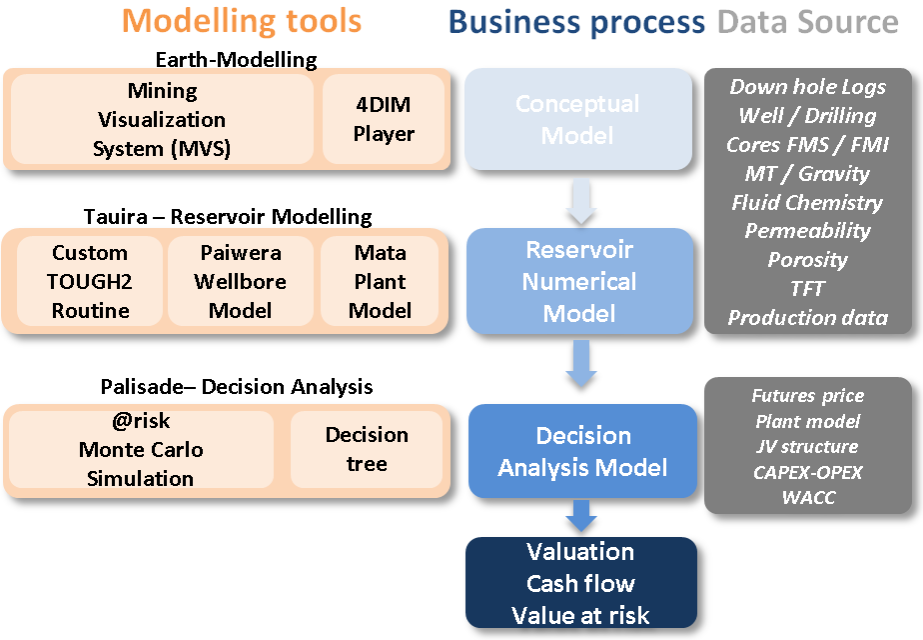

Figure 1 Modelling flow chart showing modelling tools, business process and the data used at each phase of this project

geochemistry (Addison et al., 2015a) and tracer testing (Addison et al., 2015b). In addition, a review paper (McNamara et al., 2015) provides significant information on the field. Accordingly in this paper we only give a brief description of key conceptual model features.

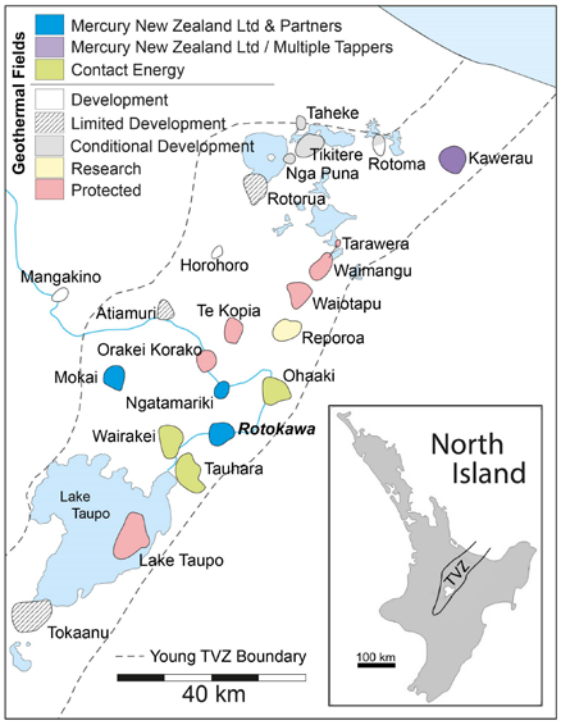

Figure 2 The location of the Rotokawa Geothermal Field in the Taupo Volcanic Zone (TVZ)

1.2 Conceptual model key features

The Rotokawa geothermal field is one of the hottest resources in the TVZ with natural state reservoir temperatures exceeding 330 °C. Temperatures differ significantly from the south to the north of the field with temperatures in the south as high as 337 °C and temperatures in the north approximately 310 °C. The field layout with well names is shown in Figure 3.

A striking feature of the reservoir is its heterogeneous pressure drawdown in different regions in response to production (Hernandez et al., 2015b). In some regions of the reservoir the drawdown is over 40 bar while in other regions it is less than 5 bar. This behaviour of reservoir pressure is often referred to as 'compartmentalization' or a 'compartmentalized' reservoir, whereby different regions of the reservoir are poorly connected. Several reservoir compartments have been identified at Rotokawa. The compartments are reasonably well understood and are generally consistent with geologic structure. Understanding the compartmentalized behaviour has been essential to obtaining a numerical model that adequately matches the pressure and enthalpy behaviour measured following the start of the Nga Awa Purua power station (Hernandez et al., 2015a).

The Rotokawa reservoir had a strong geochemical gradient across the reservoir in its natural state from the south to the north of the field. In general, the natural state reservoir geochemistry was progressively more dilute and lower gas from south to north (e.g. chloride contents varied from ~900 ppm in the south to ~450 pm in the north). Since the start of the NAP plant in 2010, the geochemistry of production wells has changed with several areas of the reservoir showing significantly different geochemistry over time (Addison et al., 2015). The different geochemistry behaviour across the reservoir generally reflects the compartmentalized nature of the reservoir and the resultant variations in boiling, dilution and injection returns (Addison et al., 2015).

Geologic structure appears to have a strong influence on fluid flow in the reservoir. One key geologic structure in the reservoir is the Central Field Fault which inhibits flow of injected fluid back into the production areas (Sewell et al., 2015b). The Production Field Fault in the western area of the reservoir also appears to be a significant geologic structure that influences reservoir hydrology (Sewell et al., 2015a). Wells RK17, RK26, RK27 and RK32 all produce from a high permeability region along the strike of the Production Field Fault. It is thought that this fault is responsible for the compartmentalized behaviour of this region of the reservoir (the Western Compartment).

2 COOLING IN THE WESTERN COMPARTMENT

The Production Field Fault is the structural control on a region known as the Western Compartment (Figure 3). Wells that produce from the Western Compartment are RK17, RK26, RK27L2, RK28 and RK32, all shown in Figure 3 . Several years after the commissioning of the Nga Awa Purua plant some wells in the Western Compartment experienced dilution and enthalpy decline. At first, this was observed mostly as geochemical dilution. This initiated a pressure, temperature, spinner (PTS) survey campaign to better understand the amount and location of the cooling. Geochemistry and tracer flow test (TFT) data was analysed to get better constraints on the level of dilution and enthalpy decline. Feedzone contributions and fault locations were also studied to help determine the source of the cooling.

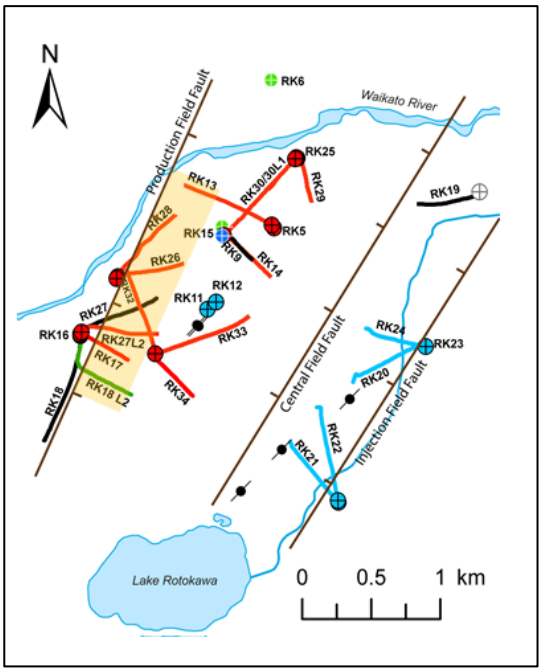

Figure 3 Rotokawa Geothermal field as at 2016 showing well locations and main faults. The Western Compartment is shown as a shaded yellow box. Production wells are shown in red and injection wells are shown in blue

2.1 Temperature, enthalpy and chloride data

As shown in Figure 4 there is clear evidence for enthalpy decline in RK17, RK26, RK27L2, RK28 and RK32. Three potential causes of this enthalpy decline were identified as cooling from marginal recharge, rise of the liquid level and/or a change in feedzone contribution over time such that wells were receiving a greater proportion of fluid from lower enthalpy feedzones. To check for changes in feedzone contribution over time, wellbore models were calibrated to PTS data and no evidence for a change in feedzone contribution was found. The liquid level decreased in the period 2010-2013 according to the pressure monitoring data available from a dedicated pressure monitoring well in the area (RK18L2) and regular static PTS runs. This ruled out a rising liquid level as a primary cause of the cooling and indicated marginal recharge as the most likely cause of enthalpy decline.

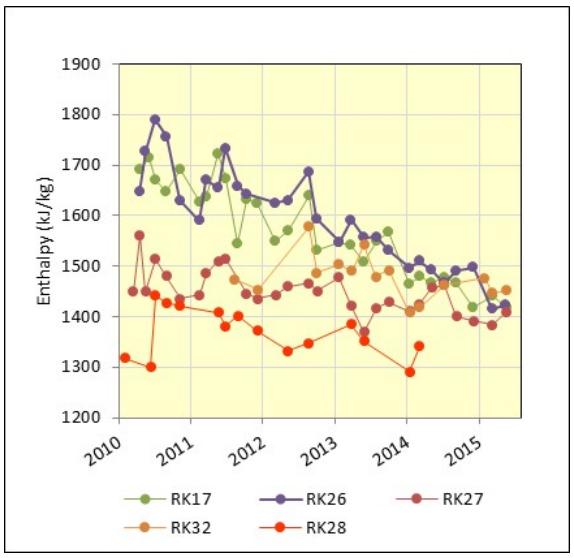

Figure 4: TFT enthalpy over time for RK17, RK26, RK27, RK28 and RK32

A flowing PTS campaign was carried out in 2014 following installation of stingers in all the wells to reduce the impact on generation. The purpose of the campaign was to compare the 2014 liquid temperature with the flowing PTS surveys carried out after completion in 2009 and in 2010.

The flowing temperature profile in RK17 conducted in 2014 was at boiling point for depth and therefore it was not possible to assess the liquid temperature. In RK27 no temperature change was observed between surveys despite the well having the second lowest enthalpy among the wells in the western compartment (Figure 4). RK26 and RK28 were the only wells showing a clear decrease in the liquid temperature (Figure 5).

The flowing PTS data showed a temperature inversion developing at around -1400 m in RK26 and RK28. In RK26 two flowing downhole surveys were used to identify the temperature and the location of the cooling which helped to infer the likely location of the source of cooling.

In 2009, after well completion, a survey showed 312 °C at -1350 masl in RK26. Another flowing PTS survey in 2014 showed a temperature of 305 °C at the same depth. It is important to highlight that the temperature at -1350 masl is the result of mixing hot fluid from -1700 masl with a colder shallower entry. Therefore, to estimate the actual location and temperature of the cooling source, a wellbore model was required. The wellbore model was constrained using the pressure, temperature, fluid velocity, production data and non-condensable gas in discharge. The best fit to all of these parameters was obtained by iteratively adjusting the parameters for each feedzone. The results in RK26 indicated a cooling source at -1400 masl with a reservoir temperature of 315ºC in 2009 and 295ºC in 2014 (Figure 5, left hand panel).

The same procedure was used in RK28. The results showed a cooling source at a very similar elevation to RK26 (-1540 masl) with the temperature decreasing from 305ºC in 2010 to 265ºC in 2015 (Figure 5, right hand panel).

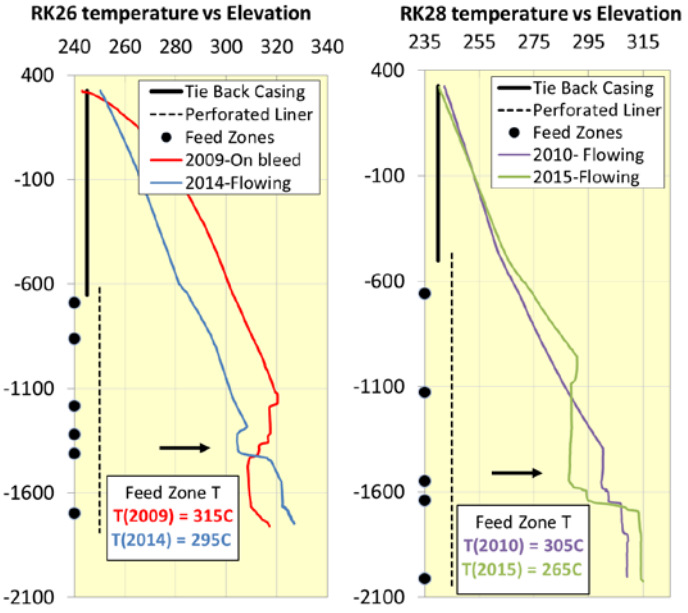

Figure 5: Wellbore flowing temperature versus elevation in RK26 and RK28. Note that temperature surveys in 2009 and 2010 were conducted following drilling and may therefore underestimate the true formation temperatures at that time.

Note that the 2009 and 2010 PTS surveys shown in Figure 5 were performed after completion when the well was still heating after drilling. It is likely that the original, natural-state reservoir temperatures for these wells were closer to the maximum measured temperatures for each of the wells (~320-330 °C for RK26 and ~315 °C for RK28).

The pressure drawdown in the period from 2009 (prior to Nga Awa Purua start-up) to mid-2015 is shown in Figure 6. This data was obtained from shut PTS surveys and a dedicated pressure monitoring well. RK28 has lower pressure drawdown than RK26 where the total drawdown is 15 bar higher. RK18L2, also shown in the figure, is a dedicated pressure monitoring well at the edge of the Western Compartment. Although RK18L2 is the lowest permeability well in the area, it is well connected to the Western compartment wells and is a good reference to indicate the pressure trend in the compartment, particularly during periods with less frequent PTS surveys (Quinao et al., 2013).

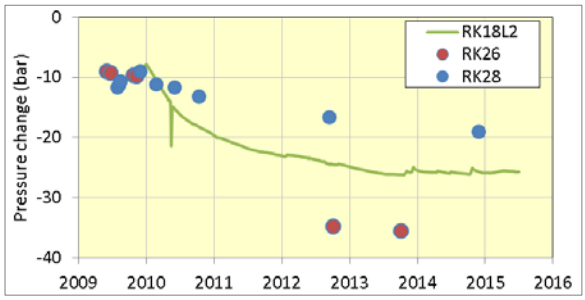

Figure 6: RK18L2, RK26 and RK28 pressure change from inferred natural state 2009-2015

The pressure has been relatively stable since 2013. This is probably due to both recharge into the compartment and a reduction in production from the compartment after the first observations of enthalpy decline. Likewise, the enthalpy decline rate in the Western Compartment has decreased in the last two years, responding positively to a reduction in take.

The change in enthalpy was also associated with a change in chloride concentration over time. A decrease in chloride generally indicates dilution with a low chloride marginal water and an increase in chloride concentration indicates boiling. Figure 7 shows a contour plot of reservoir chloride within the field, demonstrating a steep gradient in chloride between the wells showing clear signs of dilution (RK13, RK26 and RK28) and those that show signs of boiling (RK17 and RK27L2). In addition, reservoir sulfate levels are elevated in the wells seeing dilution as shown in Figure 8. This is likely due to either the ingress of naturally higher sulfate fluids or from cooler fluids that have solubilized reservoir anhydrite on their way to production. Reservoir tracer testing at Rotokawa, as discussed in Addison et al. (2015b), confirms the lack of injection returns to the wells with high chloride fluids (RK17 and RK27L2) and to the wells seeing dilution, thereby discarding injection fluids as the source of cooling in the Western Compartment.

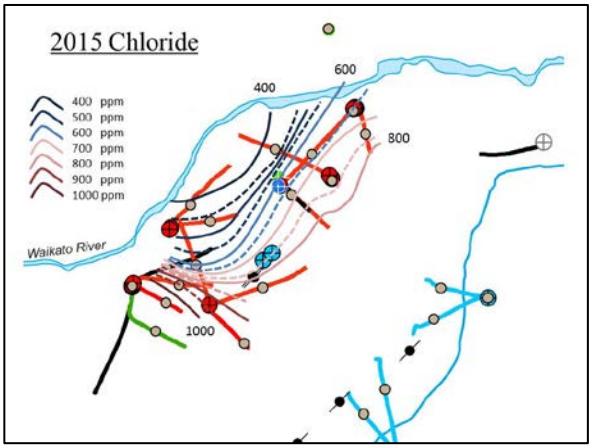

Figure 7: Reservoir Chloride for 2015 from Addison et al. (2015a).

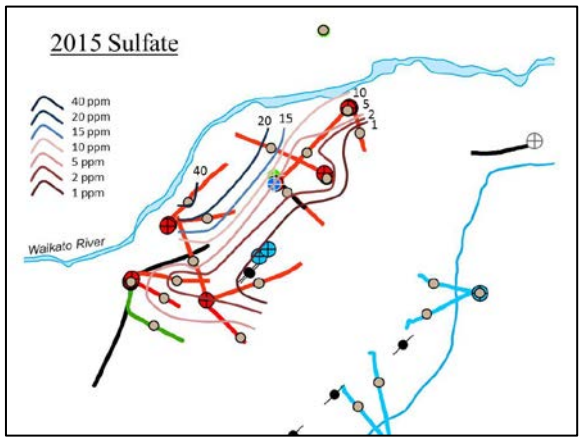

Figure 8: Reservoir Sulfate for 2015 from Addison et al. (2015a).

3 CONCEPTUAL MODEL OF THE WESTERN COMPARTMENT

After collating and analyzing reservoir data the next step in in the model-based decision making was to develop a robust conceptual model. The enthalpy and chloride data provided strong evidence for dilution with a cooler, low chloride fluid in the Western Compartment. The PTS data provided information on the location and timing of the cooling, indicating it was occurring predominantly at -1400masl with the greatest impact at RK26 and RK28.

The exact location of the source of cooling was not fully constrained by the data. There are two main possibilities; either the cooler fluid flows laterally into the compartment from the north or cooler fluid from above the reservoir is percolating down into the reservoir, possibly along the Production Field Fault.

In either case though, multiple forms of evidence indicate that the source of cooling is north of RK28. Key evidence includes: the fluid temperature (lower in RK28 than RK26); the pressure trend (more pressure support in RK28 than RK26); the reservoir chloride concentration gradient; and, the higher sulfate concentration in RK28. Similar chemistry and temperature gradients were observed in the pre-production surveys. It is considered likely that the Production Field Fault provides good permeability along its NE-SW strike, and that this therefore allows northern recharge to be channeled into the reservoir, once the pressure decreases as a result of the production.

Consistent with the conceptual understanding of the reservoir, the numerical model was built with a source of cold fluid ~2 km north of RK28. The location, temperature and flow rate of the source was varied to calibrate the model to measured data. At this stage, the downflow model has not been tested, however, it is expected that modelled outcomes would be similar to the lateral recharge model.

4 NUMERICAL MODEL CALIBRATION AND SIMULATION

In order to decide on the best strategy to optimize production but maintain the long term sustainability of the resource a tool was need to predict future reservoir behavior under various operational scenarios. The existing full field numerical model was well matched to most field data but it

did not include the cooling and enthalpy decline observed in the Western Compartment. Rather than update the full field model directly the decision was made to develop a sector model of the Western Compartment to understand the reservoir processes in this area in more detail. The grid used for this model is shown in Figure 9. This facilitated greater spatial discretization within the compartment, faster model development, shorter model run times and the inclusion of multiple fluid types to explicitly match the model against chloride data. For comparison, the sector model used in this study covered an area of 10 square kilometers while the full field model covers are area of 131 square kilometers. This sector model could then be a key input into a full field numerical model update in the future.

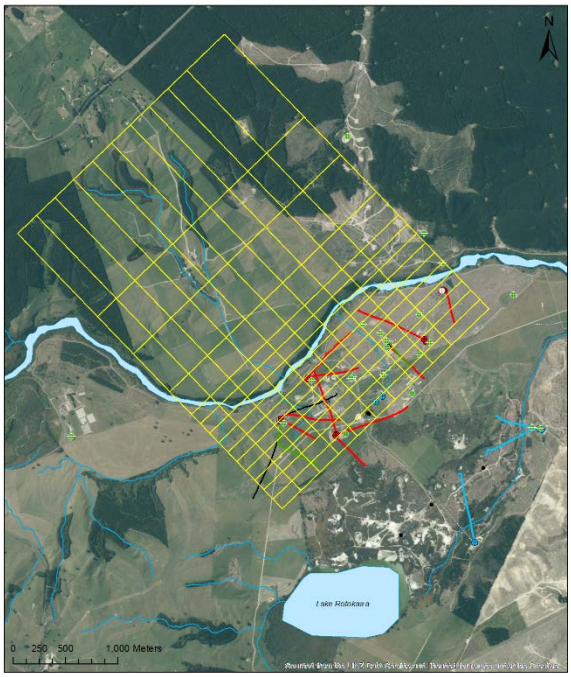

Figure 9: Model grid and field well locations. Production wells are in red and injection wells are in blue. The model is aligned with the Production Field Fault and covers sufficient area to the NW of the main reservoir for possible marginal recharge

4.1 Model description

A rectilinear model grid covering an area 3650m by 2750m was set up to cover the Western Compartment and the hypothesized recharge pathway (Figure 10). The model top was set at an approximate ground surface height of 300masl and the base was at -3500masl. Horizontally the grid was split into 14 cells in the east-west and 10 cells in the north-south direction. Vertically the model was split into 14 layers giving a total of 1960 primary grid elements.

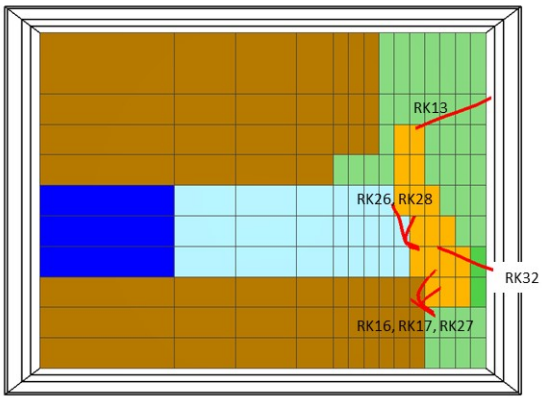

Figure 10: A horizontal slice through the model at -1400m. Wells are shown in red. Regions are the: Western Compartment (yellow), marginal recharge (dark blue); recharge pathway (light blue); low permeability rock (brown); main reservoir rock (green)

The model was originally run in TOUGH2 using EOS7 (water, brine, air) to enable a direct comparison to the chloride data.

4.2 EOS7 Natural State

The model was run to a stable state that reproduced the thermodynamic conditions of the geothermal reservoir, prior to the start of production from the area in 2010. This was indicated by a reasonable match to temperature, pressure and chloride reservoir data from 2010. Between 1997 and 2010, operation of the Rotokawa Geothermal Plant dropped the pressure in the deep reservoir by approximately 10 bar. Accordingly, the "natural state" of the model was calibrated to be 10 bar lower than pre-development pressure to represent reservoir conditions just prior to the startup of Nga Awa Purua and prior to the start of production from the Western Compartment. Mass and heat inputs into the model in the natural state consisted of a 22 kg/s upflow of 1600kJ/kg enthalpy into the base of the Western Compartment and 2.4 kg/s of 160 kJ/kg marginal recharge on the western edge of the model at -1400 m. The combination of these source terms and reservoir permeabilities were found to give a reasonable match to pressure and well temperatures. The upflow consisted 625 ppm chloride in order to match the chloride distribution in the reservoir as measured in 2010. In the natural state all fluid exited the Western Compartment vertically and flowed through an intermediate aquifer and into a fixed state block at the surface of the model. Example model comparisons are shown for chloride in Figure 11 and temperature in Figure 12.

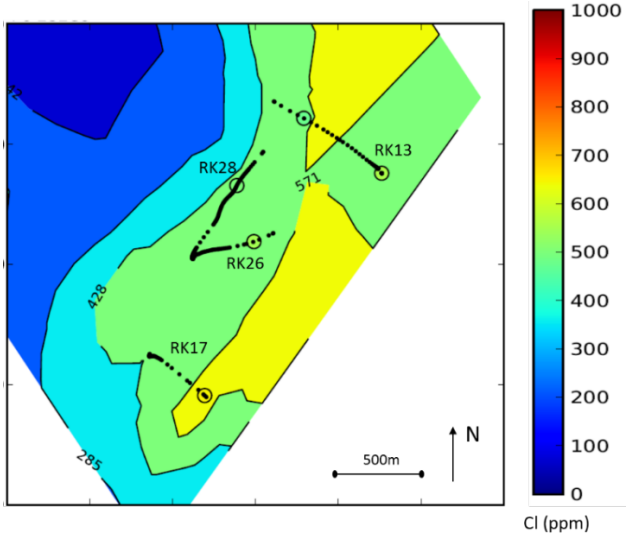

Figure 11: Modelled reservoir chloride concentration at -1400m elevation. Well tracks are shown in black. Measured data is shown as circles located at well feedzones. These are coloured by measured chloride concentration in 2010.

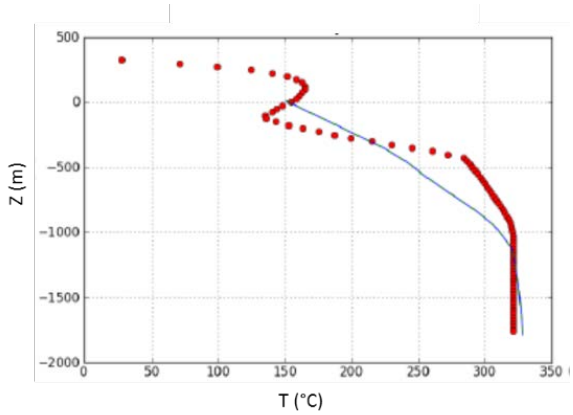

Figure 12: RK26 2010 temperature comparison. Model output is blue and interpreted natural state temperature is red

4.2 EOS7 Model production history

During the production history the marginal recharge elements were set to be fixed pressure elements. This meant that the marginal recharge flow increased as pressure declined in the reservoir to simulate the dilution observed over time. Production mass flows for each well were set by the historical field data. For each well, the feedzone locations were determined by analysis of PTS data. Feedzone allocations were determined by a coupled wellbore simulation using in-house software developed at Mercury. In this system the pressure and enthalpy at each feed was read from the numerical model and then the wellbore model was run to determine appropriate flow from each feedzone. Individual wellbore models for each well had been calibrated against PTS data. This ensured that the productivity index value used for each feedzone was appropriate which ensured the feedzone allocation was reasonable.

The calibration data for the model was the TFT enthalpy, chloride concentration, reservoir pressure and change in well temperature profile over time. Combining these data gave good constraints on the amount, general location and enthalpy of the marginal recharge to the system. The priority for model calibration was to match the mass weighted average enthalpy from the production wells. The model obtained a very close match to the enthalpy decline as shown in Figure 13.

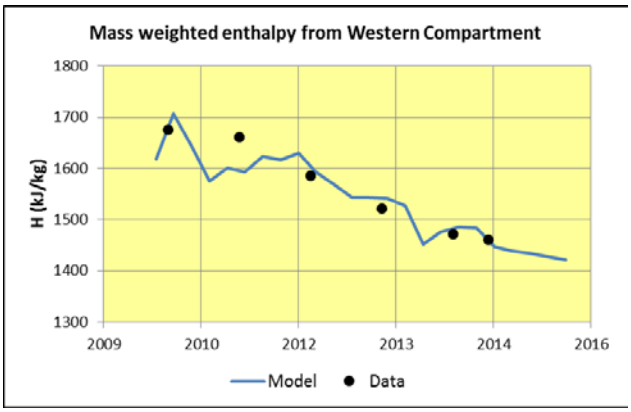

Figure 13: Mass weighted average enthalpy of wells from the Western Compartment

The match to the modelled pressure drawdown was reasonable but an exact match to the chloride data for all wells was not obtained. An example of this is shown in Figure 14 where the model closely matches the data in 2014 and 2015 but the earlier sequence is not reproduced. In this example the mismatch between observed and modelled chloride between 2010 and 2012 is likely a result of the high variability in chloride caused by variations in boiling within the compartment.

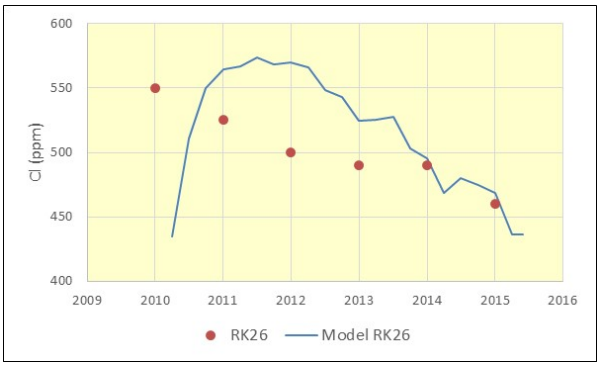

Figure 14: RK26 Chloride data (red) vs modelled (blue)

In order to match the pressure and enthalpy data and to be consistent with the chloride changes it was found that the cool marginal recharge into the system had to increase from 2.4 kg/s at the start of 2010 up to 80 kg/s at the end of 2015. The EOS7 Model was developed as a single porosity model in order to facilitate development time. For sensitivity analysis and forecast scenarios it was necessary to run the model with separate fracture and matrix elements to properly capture the physics of cooling from marginal recharge. When the EOS7 model was run as a MINC model the simulation became unstable. Attempts to debug this in a short amount of time were unsuccessful so the decision was made to simplify the modelling task by not including chloride in the simulations. The model was reformulated as an EOS2 (water, CO_2) model. The bulk of the calibration

process had been completed in EOS7 so the chloride data was still included as a constraint on the model.

4.3 EOS2 Model Scenarios

The quality of the match to natural state data of the EOS2 Model was equivalent to the EOS7 model. In recalibrating the EOS2 model we needed to fine tune the MINC parameters, it was found that a fracture volume of 0.6% and a fracture spacing of 100m gave a reasonable match to measured pressure, enthalpy and temperature change. The model match to temperature change is shown in Figure 15 and model matches to pressure and enthalpy are included in the forecasts in Figure 16 and Figure 17. The measured temperatures shown in Figure 14, correspond to the two flowing surveys carried out in RK26 and RK28 described in Section 2.1. They were estimated as the equivalent liquid temperature of the enthalpy at the feed zones at -1400 masl and -1540 masl.

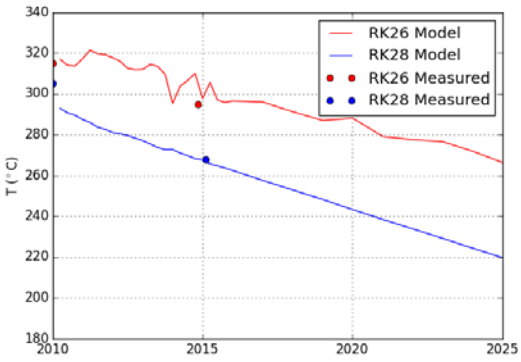

Figure 15: Modelled fracture temperature at -1400masl compared with fluid temperature estimated from wellbore model.

To help determine a field strategy the calibrated EOS2 model was used to forecast reservoir evolution under various operating conditions. In all scenarios the reservoir model was coupled to wellbore models so that the feedzone contribution changed as reservoir conditions changed and also a deliverability curve was calculated for each well over time to assess total production capacity. The scenarios run with the model were:

- ***Prod constant***: Production flows held at 2015 level
- ***Prod halved***: Production flows half of 2015 level
- ***Prod reduced:*** Production flows reduced by 30% with main reduction from RK26
- ***Prod increased***: Production flows increased by 20% with additional flow from RK28

Of the scenarios, one was run as a base case ("Prod constant"), with two scenarios run with varying levels of production reduction in the Western Compartment ("Prod halved" and "Prod reduced"). Another scenario was considered whereby RK28 could be used as a well to absorb the effects of the main inflow of marginal recharge ("Prod increased"). In this scenario RK28 could be used for purposes other than electricity generation to eliminate any enthalpy impact on the power plant operations, whilst the other wells in the compartment would have continued to supply the power plants on the field.

Results from scenarios runs are presented in Figures 16 to 19. There are two trends worth noting in the mass weighted enthalpy shown in Figure 16. The first is that reducing production from the Western Compartment causes an initial decrease in the enthalpy of the produced fluid. The second is that reducing production from the Western Compartment causes a reduction in the rate of enthalpy decline.

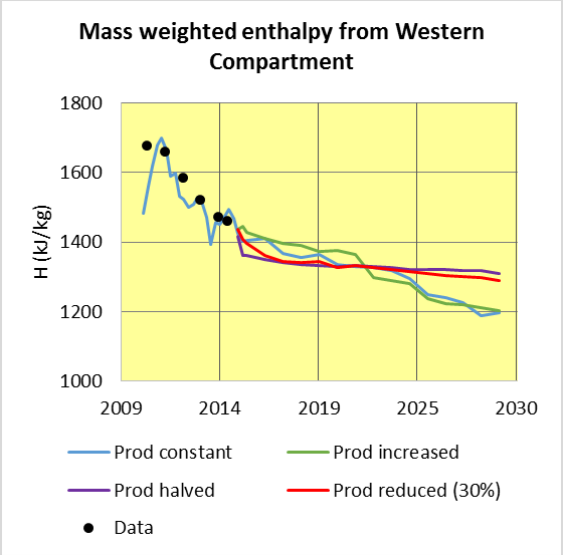

Figure 16: Mass weighted enthalpy from the Western Compartment for scenarios

The pressure response of the reservoir is shown in Figure 17. Pressure drawdown is well correlated with the total take in the compartment (i.e. the pressure decline can be mitigated by reducing the total take by 30%) such that reducing production reduces the pressure drawdown. Similar results are shown in Figure 18 where the amount of marginal recharge scales with the pressure drawdown. The pressure and marginal recharge results make intuitive sense – the more production from the Western Compartment the greater the pressure drawdown which creates a greater pressure differential to pull in more cool marginal fluid.

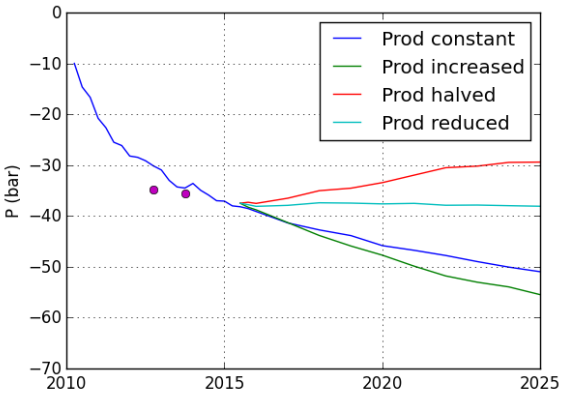

Figure 17 Pressure change in RK26 during forecast

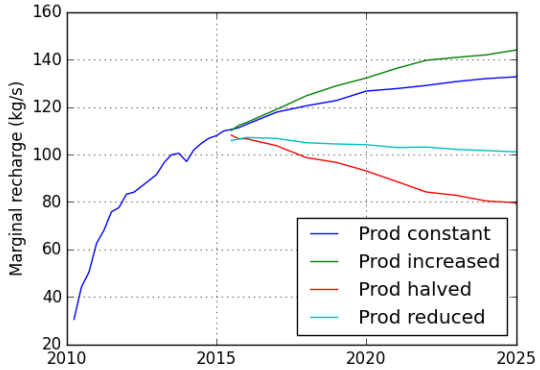

Figure 18: Quantity of marginal recharge in forecast scenarios

Because the wells were coupled to a wellbore model during production scenarios full deliverability curves were generated for each well at each time step of the forecast. It was therefore possible to look at a production capacity normalized to operating wellhead pressures. This capacity forecast is presented in Figure 19, showing that reducing production from the compartment provides for additional capacity.

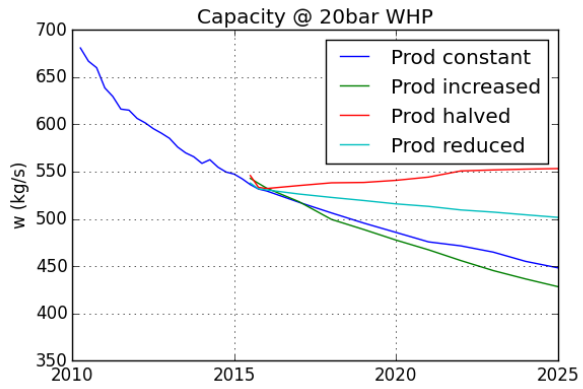

Figure 19 Total capacity of Western Compartment normalised to 20 bar well head pressure

5. DECISION ANALYSIS MODEL

The results of the previous data analysis, conceptual model development, numerical model calibration and coupled wellbore model simulations gave a forecast mass flow and enthalpy at a given wellhead pressure under various operational strategies. The results so far indicated that a reduction of the total take from the Western Compartment would cause an initial reduction in production enthalpy and then a reduction in enthalpy decline rate in the longer term. They also demonstrated that a reduction in take improved the production capacity, thus potentially reducing the need for future makeup well drilling. These benefits came at the cost of a reduction in mass produced. In contrast, maintaining a constant mass production from the Western Compartment was detrimental to the long term enthalpy forecast and the loss in production capacity could either lead to a loss in generation or the requirement to drill additional makeup wells earlier. These tradeoffs in each operational strategy were investigated in a Decision Analysis (DA) model.

A DA model, coupling the power plant operation curves, corporate financial information and forecasts of production and injection well performance was developed in Excel to calculate the free cash flow and Expected Net Present Value (ENPV) of each scenario. The capacities, enthalpies and decline rates of wells in the Western Compartment were taken from the numerical model forecasts. For wells outside the Western Compartment these forecasts were estimated by fitting an exponential curve to historical production data.

The total take required from the power plant was calculated as a function of the production enthalpy using the plant characteristic curve shown in Figure 20 (red line). As can be seen the power output and required mass flow are both sensitive to enthalpy. The DA model was run for twenty years with time-steps of one month. Well capacities and enthalpies were calculated each month by applying the corresponding decline rate. Total well capacity was compared with the power plant requirement at the given enthalpy using the characteristic curve. If the total capacity did not meet the total take required, a new make-up well was automatically added.

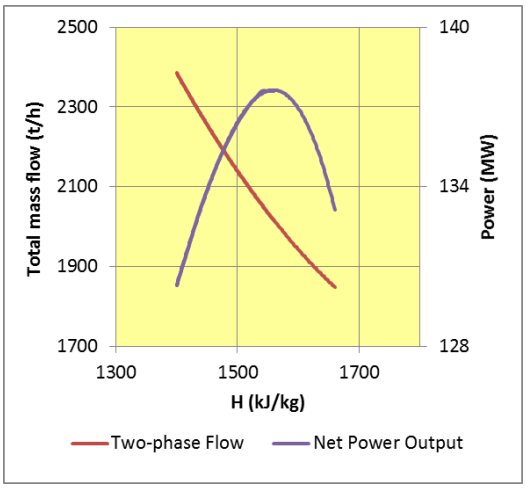

Figure 20 Characteristic station curves for Nga Awa Purua showing power output sensitivity to enthalpy (modified from Hoepfinger et al, 2015 and also the change in mass flow required with a changing enthalpy.

The income from generation was calculated using the power plant electricity generation, the expected availability, the electricity pool price and the hedging strategy. Operational costs such as future well repairs or royalty schemes were deducted from the total income to calculate earnings before interest, taxes, depreciation and amortization (EBITDA). Capital expenditures (CAPEX) were allocated when a make-up well was required (including materials and pipeline). CAPEX was deducted from the earnings after tax to calculate the free cash flow. Future cash flows were discounted to the present using the appropriate weighted average cost of capital.

A stochastic approach was used to deal with the underlying uncertainties in the forecast enthalpies and future costs for new wells. An Excel Add-in called @risk distributed by Palisade was used to define the probability distribution functions (PDF) used as inputs. Pert distributions were used to define the existing and future wells decline rates and capacities. Pert distribution were selected because they made intuitive sense given our understanding of the data and they were able to closely approximate both normal and

lognormal distributions. Discrete probability distributions were used to represent probability of success (POS) of new wells. POS was defined as the probability of obtaining the expected mass flow in the first drilling target it had a negative correlation with the drilling cost and a positive correlation with well capacity in our DA model.

The four scenarios described in Section 4.3 were analyzed using the DA model. The result of the Monte Carlo simulation was the PDF of the ENPV and therefore it was possible to express the result in terms of upside potential and downside risk. Although the full details and output from this analysis are commercially sensitive and therefore are not reproduced here, the results indicated that the optimum potential risk/benefit ratio for Mercury was achieved by reducing the take by ~30% in the Western Compartment, mainly from RK26 and RK28. This provided a more stable enthalpy in the long term, reducing the frequency of future drilling and maintaining the current levels of electricity generation.

6. CONCLUSION

This paper documents the process from identification of enthalpy decline right through to scenario forecasts that underscored a change in reservoir management strategy. The model-based approach to decision making allowed various scenarios to be explored and for these to be analysed quantitatively in terms of reservoir health, finances and generation. Several key ingredients enabled us to rely on the model as a decision making tool. These included robust data sets to calibrate the model against, a comprehensive conceptual understanding of the reservoir processes and a suite of reservoir modelling tools to enable coupled wellbore and surface facility (i.e. power plant) network simulation and fast model development. The outcome of the modelling was a modification to the reservoir management strategy to reduce take from the Western Compartment and to target future make-up production wells from areas outside of the compartment.

ACKNOWLEDGEMENTS

The authors wish to sincerely thank the Rotokawa Joint Venture (Mercury and Tauhara North No.2 Trust) for permission to publish this paper.

REFERENCES

Addison S.J., Winick, J.A., Sewell. S.M., Buscarlet, E.F.J., Siega, F.L. & Hernandez, D. (2015a) Geochemical Response of the Rotokawa Reservoir to The First 5 Years of Nga Awa Purua. Proc. NZ Geothermal Workshop.

Addison S.J., Winick, J.A., Mountain, B.W. & Siega F.L. (2015b) Rotokawa reservoir tracer test history. Proc. NZ Geothermal Workshop.

Burnell, J. (2011). Rotokawa Numerical Modelling. Industrial Research Limited Confidential Report to Mighty River Power.

Franz P. (2015) Paiwera-A robust wellbore simulator for geothermal applications. Proc. NZ Geothermal Workshop.

Franz P. (2016) MataTauira: A Growing Software Package for Numerical Geothermal Reservoir Simulations. Proc. NZ Geothermal Workshop.

Hernandez D., Clearwater J., Burnell J., Franz P., Azwar L. & Marsh A. (2015a) Update on the Modelling of the Rotokawa Geothermal System: 2010 – 2014; World Geothermal Congress, Melbourne, Australia.

Hernandez, D., Addison, S., Sewell, S., Azwar, L. & Barnes, M., (2015b). Rotokawa reservoir response to 172 MW of geothermal operation. Proc. New Zealand Geothermal Workshop, Taupo.

Hoepfinger, Z., Marsh, A., and Maginness, R. (2015) Adopting surface facilities to changes in Rotokawa reservoir in the first 5 years of Nga Awa Purua, New Zealand Geothermal Workshop.

McNamara, D., Sewell, S., Buscarlet, E., & Wallis, I. (2015) A Review of the Rotokawa Geothermal Field, New Zealand. Geothermics.

Sewell, S. M., Addison, S., Hernandez, D., Azwar, L. & Barnes, M. (2015a) Rotokawa Conceptual Model Update 5 years After Commissioning of the 138 MWe NAP Plant. Proc. NZ Geothermal Workshop, Taupo.

Sewell, S. M., Cumming, W., Bardsley, C., Winick, J., Quinao, J., Wallis, I., Sherburn, S., Bourguignon & S., Bannister, S. (2015b). Interpretation of microseismicity at the Rotokawa Geothermal Field, 2008 to 2012. Proc. World Geothermal Congress, Melbourne, Australia.

Quinao J, Azwar L., Clearwater J., Hoepfinger V., Le Brun M. & Bardsley C. (2013) Analyses and modeling of reservoir pressure changes to interpret the Rotokawa geothermal field response to Nga Awa Purua power station operation Proceedings, Thirty-Eight Workshop on Geothermal Reservoir Engineering Stanford University, Stanford, California

Winick, J., Powell, T. & Mroczek, E. (2011) The Natural State of the Rotokawa reservoir. Proc. New Zealand Geothermal Workshop.